Available online at www.sciencedirect.com
SCIENCE DIRECT
Journal of Power Sources 154 (2006) 298–307
JOURNAL OF POWER SOURCES
www.elsevier.com/locate/jpowsour

New dry and wet Zn-polyaniline bipolar batteries and prediction of voltage and capacity by ANN

Hassan Karami [a], Mir Fazlollah Mousavi [a,*], Mojtaba Shamsipur [b], Siavash Riahi [a]

[a] *Chemistry Department, Tarbiat Modarres University, P.O. Box 14115-111, Tehran, Iran*
[b] *Chemistry Department, Razi University, Kermanshah, Iran*

Received 2 November 2004; accepted 1 April 2005
Available online 8 June 2005

Abstract

Chemically synthesized polyaniline doped with perchlorate ion was used as the electroactive material of the cathode in the construction of bipolar rechargeable batteries based on carbon doped polyethylene (CDPE) as a conductive substrate of the bipolar electrodes. A significant improvement in the originally poor adherence between the polymer foil and electroactive material layer of the anode was achieved by chemical pretreatment (etching) and single-sided metallization of the polymer foil with copper. A thin layer of optalloy was electroplated onto the surface of the copper-coated polymer foil to increase the battery overvoltage. A mixture of 1 wt% electrochemically synthesized optalloy, 92 wt% electrochemically synthesized zinc powder, 2 wt% MgO, 4 wt% ZnO and 1 wt% sodium carboxymethyl cellulose (CMC) was used as the anode mixture. Then, the electroactive mixture of the anode was coated onto the metallized surface of the CDPE. Graphite powder was used to coat the other side of the CDPE at 90 °C at 1 t cm^{-2} pressure This side was coated with a cathode mixture containing 80 wt% polyaniline powder, 18 wt% graphite powder and 2 wt% acetylene black. The battery electrolyte contained 1 M $Zn(ClO_4)_2$ and 0.5 M NH_4ClO_4 and 1.0×10^{-4} M Triton X-100 at pH 3.2. Both 3.2 V dry and wet bipolar batteries were constructed using a bipolar electrode and tested successfully during 200 charge–discharge cycles. The battery possessed a high capacitance of 130 mAh g^{-1} and close to 100% columbic efficiency. The loss of capacity during charge–discharge cycles for the wet bipolar battery was less than that for the dry bipolar battery. Self-discharge of the dry and wet batteries during a storage time of 30 days was about 0.64% and 0.45% per day, respectively. An artificial neural network (ANN) was used to model the voltage and battery available capacity (BAC) only for the dry bipolar battery at different currents and different times of discharge.

Keywords: Rechargeable bipolar battery; Zn-polyaniline; Carbon doped polyethylene (CDPE); Battery available capacity (BAC); ANN modeling; Simultaneous prediction

1. Introduction

Recently, considerable interest has been paid to the study of polyaniline as a cathode in rechargeable batteries [1–6]. The majority of previously reported polyaniline-based rechargeable batteries are of the wet-type, in which hydrochloric acid or sulfuric acid have been used as a dopant acid and the corresponding electrolyte solutions contain $ZnCl_2$ and NH_4Cl at pH 4 and higher [7–11].

Recently, the use of bipolar systems in the construction of batteries has increased [12–16]. An important parameter in high-energy batteries is the thickness of the electrodes. Bipolar, flat plate electrodes demonstrate the importance of this parameter. The application of a bipolar cell design offers several advantages [13] and, therefore, this structure is used in the design principle for modern batteries. The design principle is strongly influenced by the choice of the electrochemical couple of the storage system [13].

Various substrates including stainless steel, lead, silver and carbon-polymer composite foils have been used in the construction of bipolar electrodes [14,17–22]. The aggravating disadvantages in the use of plastics as carriers for electroactive materials include low conductivity and lack of adherence to the electroactive layers. Usually, the electroactive materials are deposited onto the surface of a conductive

* Corresponding author. Fax: +98 21 8006544.
E-mail address: mousavim@modares.ac.ir (M.F. Mousavi).

0378-7753/$ – see front matter © 2005 Elsevier B.V. All rights reserved.
doi:10.1016/j.jpowsour.2005.04.002

carrier (metal or conductive polymer). A significant improvement of the originally poor adherence of the polymer foil to the electroactive layers can be achieved by mechanical (surface roughening) or chemical (etching) pretreatments [18–20].

The use of plastics with conductive fillers, like graphite and/or soot incorporated into the polymer demands an intermediate layer between the carbon-filled polymer and the zinc to prevent the formation of hydrogen gas by anodic corrosion, which is enhanced in the presence of carbon in any modification. The use of intrinsically conductive polymers like polypropylene and polyethylene as carrier materials requires special precautions and manufacturing processes because most of these polymers are insoluble and brittle. Thus, further treatment is hardly practicable. The advantage of intrinsically conductive polymers compared with filled plastics is that an intermediate layer between the carrier and the zinc is unnecessary. The achievable resistance of both plastics with conductive fillers and intrinsic conductive polymers are not comparable to that of metal carriers. However, the achievable resistance is sufficient for thin foils in bipolar arrangements.

Another promising method to form extremely thin electrodes, with a thickness in the range of some ten micrometers, is as follows:

- A metallic layer, serving as a current collector, is deposited onto one side of a thin, porous polymer foil such as polyethylene or polypropylene [18].
- The electroactive material is electrolytically or mechanically deposited onto the surface of a metallized plastic [19].

The flexibility of the polymer has a positive influence on the volume change of electroactive materials because the plastic provides flexible ‘mechanical struts’. The plastic acts as a binder and, therefore, prevents an increase in the internal resistance due to contact problems.

In previous studies, we employed polyaniline in the construction of a rechargeable battery [23], and showed that the polyaniline doped with perchlorate acts as a more suitable cathode material than chloride doped polyaniline for use in dry rechargeable batteries [24]. Recently, we successfully designed and constructed a rechargeable Zn-polyaniline dry battery based on stainless steel bipolar electrodes [12].

In all types of batteries, battery voltage is the first and most important factor. Modeling and prediction of voltage at various times and currents of discharge for each type of battery are of special interest. Because of the non-linear relationship between battery voltage and time of discharge and also voltage and discharge currents, artificial neural networks (ANNs) seem to be the most suitable for such modeling processes. In recent years, multivariate methods and ANNs were used for the prediction of battery characteristics such as capacity [25–30].

In order to fully employ the stored energy of the batteries, the accurate determination of battery available capacity (BAC) is very important. To the best of our knowledge, there are no reports about the modeling and prediction of polyaniline batteries. Most reports regarding modeling and prediction of battery characteristics were about lead-acid batteries [25–30]. For lead-acid batteries, the Peukert equation approach, which describes the relationship between the BAC value and the discharge current (I_d), is most commonly adopted. The Peukert equation is expressed as [31,32]:

$$\mathrm{BAC} = \frac{k}{I_d^{(n-1)}} \tag{1}$$

where k and n are constants determined from the discharge data of the lead-acid battery. However, the accuracy of the calculated BAC from Eq. (1) decreases drastically at both low and high discharge currents. Recently, a multi-level Peukert equation has been developed to improve the calculated accuracy, where two sets of constants k and n were specifically adopted for the calculation of the BAC under low and high discharge currents [27]. Nevertheless, Peukert-based equation approaches are only valid for lead-acid batteries and are ill suited to other batteries. To meet this purpose, BAC calculation at different discharge currents using an ANN has been proposed. This calculation can more accurately determine the BAC of other battery types, as well.

ANNs are mathematical systems that simulate biological neural networks. They consist of processing elements (neurons) organized in layers. The neural network used in this work is a back-propagation neural network (BPNN) [33–38]. A typical feed-forward neural network with back-propagation has three layers: the input, the hidden, and the output layers. The activation of a neuron is defined as the sum of the weighted input signals to that neuron:

$$\mathrm{Net}_j = \sum_i W_{ij} X_i + \mathrm{bias}_j \tag{2}$$

where W_{ij} is the weight-connection to neuron j in the current layer from neuron i in the previous layer, X_i is the input signal and bias j is the bias of neuron j. The Net_j of the weighted inputs is transformed with a transfer function, which is used to get to the output level. Several functions can be used for this purpose, but the “sigmoid function” is applied most often. This function is as follows:

$$y_j = \frac{1}{1 + \mathrm{e}^{-c\mathrm{Net}_j}} \tag{3}$$

where y_j is output of neuron j and c is a constant ($c \neq 0$). The network learns by adjusting its weights according to the error E [Eq. (4)]. The goal of training a network is to change the weights between the layers in a direction that minimizes the error E.

$$E = \frac{1}{2} \sum_p \sum_k (y_{pk} - t_{pk})^2 \tag{4}$$

The error E of a network is defined as the squared differences between the target values t and the outputs y of the output neurons summed over p training patterns and k output nodes.

ANNs have been used for the prediction of capacity and power [30,39], gust effects on a grid-interactive wind energy conversion system with battery storage [40], cycle life and battery failure [41].

In this work, new dry and wet Zn-polyaniline rechargeable bipolar batteries are reported. Perchlorate ion doped polyaniline, an electrolyte containing $Zn(ClO_4)_2$, NH_4ClO_4 and Triton X-100 at pH 3.2 and bipolar flat electrodes based on carbon doped polyethylene (CDPE)are used in these batteries. Optalloy is used in the anode mixture, which increases the overvoltage for the reduction of H^+ ions and, consequently, prevents the formation of Zn-hydrogen local cells [18]. Here, Triton X-100 is employed in the battery electrolyte to prevent zinc dendrite formation [42]., Graphite powder and acetylene black are added to the polyaniline powder to increase the conductivity of the polyaniline. Electrochemically synthesized zinc powder is mixed with magnesium oxide and zinc oxide to increase the reversibility and porosity of the zinc and sodium carboxymethyl cellulose is added to provide a suitable link joint of zinc particles.

This work shows that the conductive carbon-polymer mixture acts as a suitable substrate in Zn-polyaniline bipolar batteries and improves the capacity and columbic efficiency of these batteries. Moreover, the optalloy increases the hydrogen overvoltage, similar to mercury.

Finally, we report an artificial neural network (ANN) developed for voltage and capacity prediction by using voltage and capacity as outputs and time and current as inputs. The obtained values agreed with the experimental data.

2. Experimental

2.1. Reagents and materials

Aniline, ammonium persulfate and zinc chloride were obtained from Aldrich. All other reagents such as hydrochloric acid, sodium hydroxide and other compounds were of analytical reagent grade (Fluka or Merck). Argon gas (purity of 99.999%) was obtained from Roham Gas Co. (Tehran, Iran). CDPE was obtained from Zipperling Co. All reagents used in electroplating experiments were of industrial grade. Water used in all experiments was doubly distilled.

2.2. Apparatus

All electropolymerization reactions were carried out with a BHP 2061-C Electrochemical Analyzer (Beh-Pajoh Co., Isfahan, Iran). A potentiostat/galvanostat power supply (Afzar Azma Co., Tehran, Iran) was used in electrosynthesis and in electroplating experiments. Potential measurements were carried out with a Sa-Iran digital multimeter 8503 and pH measurements were made with a Metrohm pH-meter model 691. All electrochemical studies were carried out with an electroanalytical instrument (A273, EG&G, USA). All charge and discharge tests of batteries were carried out with a multichannel battery tester (BPT Co., Tehran, Iran).

2.3. Methods

One side of each CDPE foil was coated with graphite powder at 90 °C and 1 t cm^{-2} of pressure. This surface was used as a cathode current collector. The other side of each CDPE foil was metallized by copper electrolysis [12,19,20] and then supported by copper electroplating [12,19,20]. Brass alloy [43] and optalloy [20] were electroplated onto the copperized surface to improve the current collection characteristics and corrosion resistance in the acidic media.

Polyaniline was synthesized by chemical polymerization from a solution containing 0.10 M aniline, 2 M perchloric acid and 0.15 M ammonium persulfate at 5 °C [12]. Argon gas was passed through the polymerization solution to remove the dissolved oxygen during polymerization; the argon flow was directed over the surface of solution to prevent oxygen diffusion. After 24 h, the mixture was filtered, washed with water and 2 M $HClO_4$ and then poured into tetrahydroforan to separate the polyaniline small chains, which are soluble in tetrahydroforan. It should be noted that the presence of small chains decreases the conductivity of polyaniline. The mixture was then filtered and washed three times with 2 M $HClO_4$ and water. The resulting polyaniline was dried under vacuum at 80 °C and powdered into particles 54–73 μm in diameter by using two sieves of 200 and 270 mesh. Then, 80 g of this powder was mixed with 18 g of graphite and 2 g of acetylene black for use as the cathode of the battery [24].

Electrochemically synthesized zinc powder (92 g) was mixed with electrochemically synthesized optalloy powder [19] (1 g), magnesium oxide (2 g), zinc oxide (4 g) and sodium carboxymethyl cellulose (CMC, 1 g) and used as the anode of the battery. A solution containing 1 M $Zn(ClO_4)_2$, 0.5 M NH_4ClO_4 and 1×10^{-4} M Triton X-100 with a pH of 3.2 was used as the electrolyte of the battery. Triton X-100 was added to prevent the formation of zinc dendrites in the charge processes [42].

A program for the feed-forward neural network trained by the back-propagation strategy was written in MATLAB in our laboratory. All calculations presented in this work were carried out on a Hewlett-Packard 2.8 GHz Pentium computer model HP Vectra VL The initial weights, randomly selected from a uniform distribution, ranged between −0.3 and +0.3. The initial bias values were set to be one. These values were optimized during the training of the network. The modeling with raw data showed that there was a high prediction error. Therefore, the value of each input was mean-centered and auto-scaled. The resultant data were used in the ANN by employing a sigmoid transfer function. Before training,

the network was optimized for the number of nodes in the hidden layer, learning rates and momentum. The standard error of prediction was used to evaluate to performance of the ANN. Then, the network was trained using a training set derived from a back-propagation strategy employed for the optimization of the values of the weights and biases.

The experimental data of voltage and available capacity of each battery at different times and discharge currents were randomly divided into two groups, a training set consisting of discharge currents of 100, 150, 200, 225, 250, 500 mA and a validation set consisting of discharge currents of 175 and 300 mA with a time range of 0–1574 s. The training set was used for the construction of the model and the validation set was used for the evaluation of the model. All data in the training and validation sets were obtained at room temperature.

3. Results and discussion

Since battery efficiency is dependent on the conductivities of the cathode and anode as well as the bipolar substrate, all components used for the construction of the battery should be highly conductive. In this case, polyaniline is a limiting factor and, thus, it should be synthesized under optimum conditions in order to obtain the highest conductivity. Polyaniline conductivity depends on various parameters including the temperature during polymerization and concentrations of aniline, amonium persulfate (oxidant) and dopant acid (perchloric acid) in the synthesis solution. For this reason, the polyaniline was polymerized in a solution containing 0.1 M aniline, 0.15 M ammonium persulfate and 2 M perchloric acid at $\leq 5\,^{\circ}C$, as reported elsewhere [12,24].

Since bipolar battery efficiency is also dependent on the adhesion of the active material to the substrate, the design

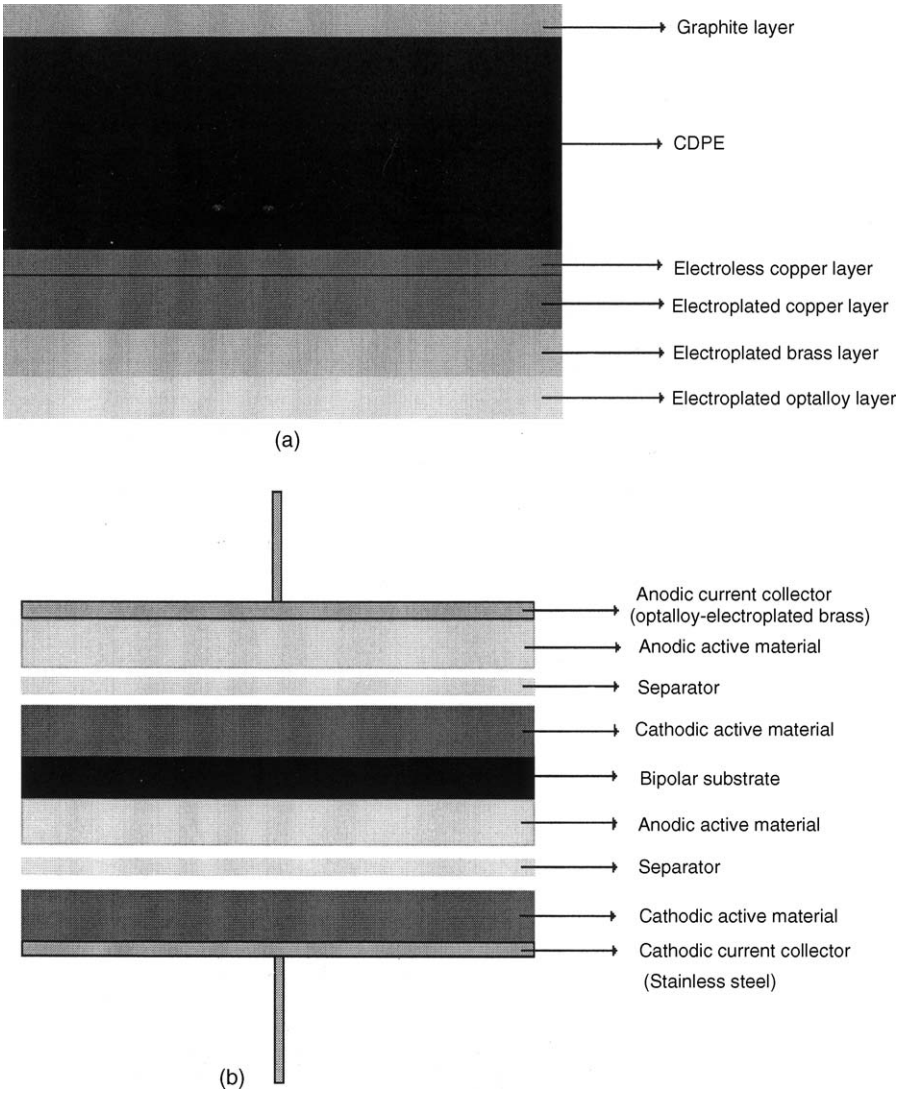

Fig. 1. Structure of the proposed bipolar battery, in which stainless steel has been used as a cathodic current collector, carbon doped polyethylene as the bipolar electrode and brass alloy as an anodic current collector. (a) Presentation of different layers of bipolar electrode substrate; (b) presentation of different parts of the bipolar battery.

and construction of the battery assembly is very important [12,17]. Thus, during the assembly of the dry battery, different battery parts should be efficiently connected to each other. For this purpose, after overlaying the battery components, we used three bolts and nuts to press them efficiently. The structure of this bipolar battery is shown in Fig. 1. In this structure, we used acid resistant stainless steel as the cathodic current collector, optalloy-electroplated brass plate as the anodic current collector and polyethylene as the cover of the battery. A CDPE foil, metallized on one side and graphite coated on other side, was used as the bipolar substrate. The assembly of the wet bipolar battery was similar to that of the dry battery except that the wet battery had a small distance between the sub-cells for filling of the electrolyte.

The battery electrolyte was composed of a solution of 1 M $Zn(ClO_4)_2$ and 0.5 M NH_4ClO_4 with a pH of 3.2. At this pH, the reversibility of polyaniline is better than at a higher pH, as reported previously [7,8,10]. To prevent zinc corrosion in the acidic media, optalloy powder was added to the anode mixture [18,20,22,24]. Optalloy is an alloy containing 55%wt Cu, 25%wt Sn and 20%wt Zn [18,20].

The influence of discharge current density on the capacity and the columbic efficiency of the dry and wet batteries was examined and the results are as shown in Fig. 2. The maximum columbic efficiency and capacity of the dry batteries were achieved at current densities of 200 mA g^{-1} and lower, with respect to the polyaniline weight. The wet batteries can be used at current densities up to 225 mA g^{-1} without losing capacity and columbic efficiency. This might be due to the lower internal resistance of wet batteries. For both wet and dry batteries, at higher current densities, only the outer layer of electroactive material can contribute to the charge and discharge process and, therefore, the battery capacity is decreased. Most types of batteries can accept larger amounts of charge current than discharge current, so by increasing

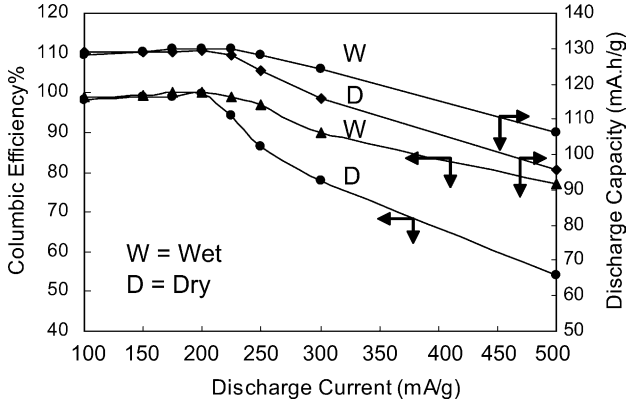

Fig. 2. (a and b) Effect of discharge current density on columbic efficiencies and capacities of wet and dry bipolar batteries.

the current density, the discharge capacity decreases more than charge capacity. Consequently, columbic efficiency is also decreased at larger current densities (i.e. >200 mA g^{-1} for dry and >225 mA g^{-1} for wet batteries). Thus, for dry and wet bipolar polyaniline batteries, the respective current densities of 200 and 225 mA g^{-1} were found to be the best operation discharge currents.

To investigate the efficiency of the dry and wet batteries, their behavior was studied during 200 charge and discharge cycles. Fig. 3(a) shows the voltage-time behavior of the dry battery during various charge and discharge cycles by the constant current method under a current density of 200 mA g^{-1} polyaniline. For comparison purposes, the wet battery was studied in the same manner as the dry battery. Fig. 3(b) compares the voltage–time behaviors of the dry and wet bipolar batteries at cycles 1 and 200. As seen in Fig. 3(b), the wet battery is more efficient than the dry battery. The variation of capacity (3) and columbic efficiency (4) of the battery were calculated by the following equations using the data obtained

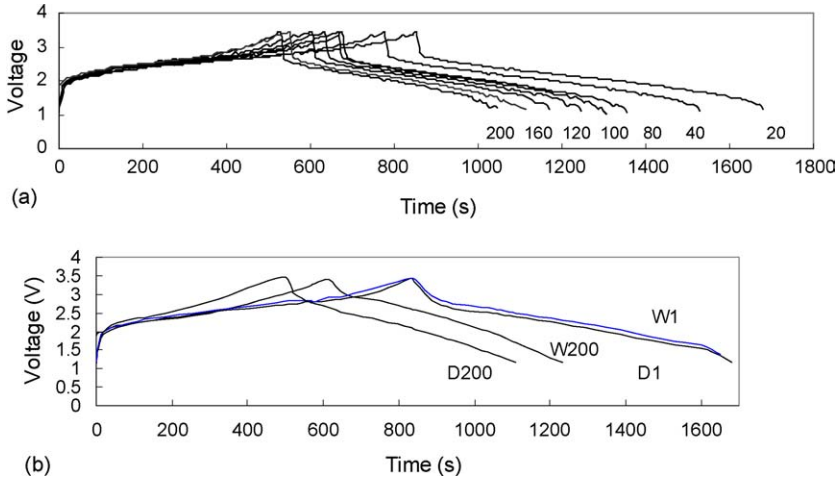

Fig. 3. (a) Voltage–time behavior of the 3.2 V dry bipolar battery during various cycles of charge and discharge by the constant current method (200 mA g^{-1}). (b) Comparison of voltage–time behaviors between dry and wet bipolar batteries at cycles 1 and 200. W_1: wet battery at cycle 1; D_1: dry battery at cycle 1; W_{200}: wet battery at cycle 200; D_{200}: dry battery at cycle 200.

from the charge and discharge cycles:

$$C = \frac{it}{w} \quad (5)$$

where C is the capacity (mAh g^{-1}), i the current (mA), t the time (h) and w is the polyaniline weight (g).

$$\text{percent columbic efficiency} = \left(\frac{t_2}{t_1}\right) \times 100 \quad (6)$$

where t_1 and t_2 are times of charge and discharge at a constant current.

Variations in discharge capacities and columbic efficiencies of the dry and wet batteries during their charge–discharge processes are shown in Fig. 4. As seen in Fig. 4, the columbic efficiencies of the batteries do not show any considerable change with the cycle number. It can be concluded that a suitable reorientation of polyaniline chains, an efficient contact between the electroactive materials and the bipolar substrate are responsible for such a favorable outcome. Fig. 4 also shows that the capacities of both dry and wet batteries decrease gradually as the number of charge–discharge cycles increases. This is most probably related to the degradation of polyaniline, which decreases the amount of active cathode material in the battery. Although the decrease in active polyaniline due to degradation in both the dry and wet batteries should be the same, the capacity loss in the dry battery is higher than in the wet battery. This is the result of the consumption of water in the process of degradation of the polyaniline [44,45]. During the charge–discharge cycles, the battery electrolyte is concentrated and, consequently, the dry battery with much less electrolyte is expected to lose its capacity faster than the wet battery with more electrolyte. The degradation reactions of polyaniline are known to require several steps [44,45], as follows:

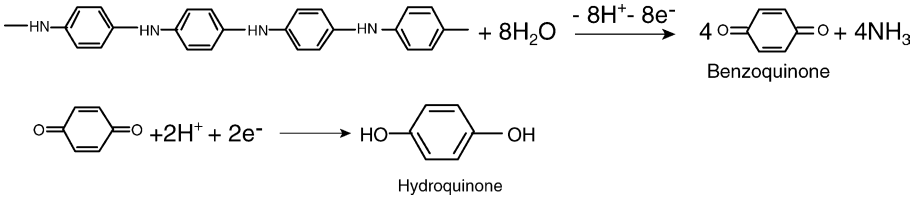

As seen in the above reaction pathway, during the degradation of each replicate unit of polyaniline in leucoemeraldine form, eight water molecules are consumed and four benzoquinones are formed in the electrolyte solution. Thus, the electrolyte becomes concentrated and each molecule of benzoquinone takes two electrons and is reduced to hydroquinone. This reaction can interfere with the main electrochemical reactions of the battery.

In our previous reports [12,24], it was clearly shown that optalloy could be used to prevent the hydrogen reduction in the anode of batteries. In this work, we studied the electrochemical behavior of hydrogen reduction on the surface of the optalloy and CDPE (Fig. 5) by linear sweep voltammetry. As seen in Fig. 5, while the hydrogen reduction begins at about −300 mV versus the Ag/AgCl reference electrode

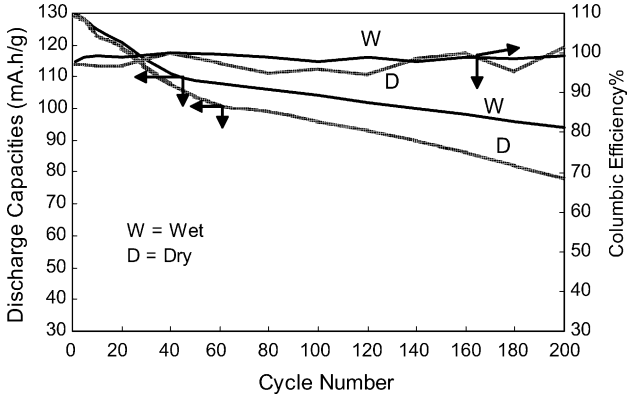

Fig. 4. Effect of cycle life on columbic efficiencies and discharge capacities of wet and dry bipolar batteries.

(curve a) on the working electrode of CDPE, the overvoltage of hydrogen reduction is increased and shifted to a negative potential of −900 mV versus the Ag/AgCl reference electrode on the surface of the CDPE metallized with optalloy (curve c). Consequently, during the battery cycle life, hydrogen cannot be reduced at the surface of the battery electrodes. This will prevent the formation of local zinc-hydrogen cells in the batteries. Mercury has been known to be a substrate with the highest overvoltage for hydrogen. In Fig. 5, curve b shows the mercury effect on the overvoltage of hydrogen reduction, and the similarity of the effect of optalloy to that of mercury. It should be mentioned that the optalloy is not toxic nor does it have negative environmental effects.

The self-discharge rate is one of the most important parameters of batteries. In order to investigate the self-discharge of the proposed dry and wet batteries, they were stored at rest for 30 days. The open circuit voltages (OCV) of these batteries were measured by a digital voltmeter every day. Fig. 6 shows the decrease in the OCVs of the dry and wet bipolar batteries with two bipolar electrodes (4.8 V) during the storage time in percent per day. As seen in Fig. 6, during the storage time, the percent of OCV reduction for the wet battery is lower than that of the dry battery. This is probably due to the fact that, in the process of preparation of the dry batteries, the cathodic and anodic active materials and the separator are assembled under pressure, which may result in the leakage of electrical current from the anode to the cathode via the separator.

With all types of batteries, voltage and capacity are very important and modeling and prediction of these parameters is of great interest. Battery voltage is reduced during the dis-

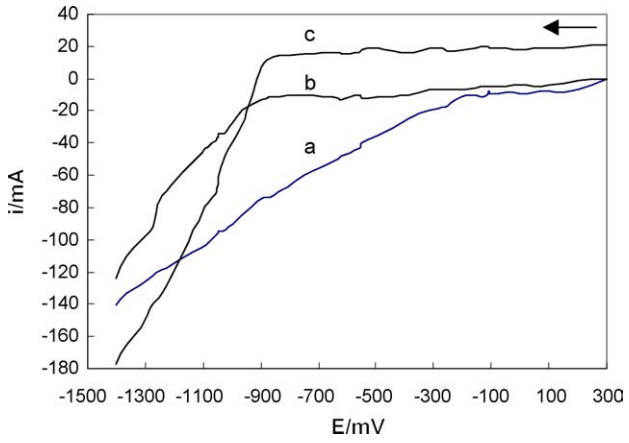

Fig. 5. Linear sweep voltammograms of hydrogen reduction on the surface of (a) CDPE in 0.5 M NH_4ClO_4 solution at pH 3.2; (b) CDPE in 0.5 M NH_4ClO_4 and 0.01 M $HgSO_4$ solution at pH 3.2; (c) optalloy coated CDPE in 0.5 M NH_4ClO_4 solution at pH 3.2.

charge process. The amount of voltage reduction depends on the current and time of discharge. By increasing the time and/or discharge current, the battery voltage will decrease.

There are many ways to define battery capacity. Among these definitions, the rated capacity (RC), state of charge (SOC) and battery available capacity (BAC) are often employed. The rated capacity is the electrical charge that the battery can deliver during the specified discharge current and a known temperature to reach the cutoff voltage. This type of capacity depends on the active mass contained in the battery and how much of this material undergoes reaction before the battery can no longer deliver the specified current at the cutoff voltage. For commercial batteries, the RC is only a reference value, which cannot be considered as the actual capacity. The SOC is defined as the ratio of the remaining active material to the total active material inside the battery. The higher the SOC, the longer the capacity can be maintained at the same discharge current. The BAC refers to the quantity of electricity that can be delivered at a certain discharge current and temperature before reaching the specified cutoff voltage. This is the most common way to define battery capacity. The BAC is strongly dependent on both the discharge current and

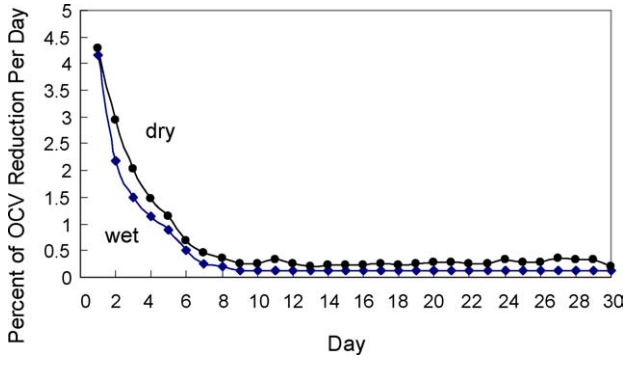

Fig. 6. Variation of OCV for the dry and wet bipolar batteries during a storage time of 30 days in percent per day.

Table 1
Architecture and specification of the generated ANN

Number of nodes in the input layer	2
Number of nodes in the hidden layer	5
Number of nodes in the output layer	2
Learning rate	0.9
Momentum	0.8
Number of epochs	10000
Transfer function	Sigmoid

temperature. The BAC decreases with increasing discharge current. There are many reasons for this phenomenon. The most important one is that at a high discharge current (rapid discharge), the electrochemical reactions take place mostly on the surface of the electrodes due to the limited time for diffusion of the electrolyte into the pores of the active material.

Because of the importance of voltage and BAC, predicting them is of great interest. ANNs are a reliable way to simultaneously model and predict voltage and BAC. To employ ANNs, they should be trained by experimental data, known as a training set. Before the training of the network, parameters regarding the number of nodes in the hidden layer, weights and biases, learning rate and the momentum should be optimized. The procedure for the optimization of these parameters has been reported previously [37]. Table 1 shows the architecture and specification of the optimized ANN used in this work. The scheme of the optimized ANN model is shown in Fig. 7. After the optimization of the ANN parameters, the network was trained using the training set for the optimization of weights and biases values. For the evaluation of the prediction power of the network, the trained ANN was used to predict the voltages and the available capacity in the prediction set. The percent of maximum error between the calculated and the experimental values of the voltage and BAC for the test set was 4.18% and 1.22%, respectively. Fig. 8(a and b) are plots of predicted voltage and BAC versus the corresponding experimental data, at a discharge current of 250 mA g^{-1} from the training set. As seen in Fig. 8, the predicted data and experimental data are in agreement. The correlation coefficients of 0.9897 and 0.9999 for the two plots confirm the ability of the ANN model to predict the voltage and BAC, respectively.

For validation of the proposed model efficiency, the model was used to predict the voltage and BAC at two different discharge currents (175 and 300 mA g^{-1}) during a discharge time of 0–1574 s. Variations in voltage and BAC versus discharge time at discharge currents of 175 and 300 mA g^{-1} are shown in Fig. 9(a and b), respectively. As seen in Fig. 9(a and b), the training of the ANN model was successful and there is agreement between the experimental and predicted data.

Fig. 10(a and b) plot predicted voltage versus corresponding experimental data at discharge currents of 175 and 300 mA g^{-1} in the validation set. Here again, the predicted data and experimental data are in agreement. The correlation coefficients of 0.9966 and 0.9884 for discharge currents of

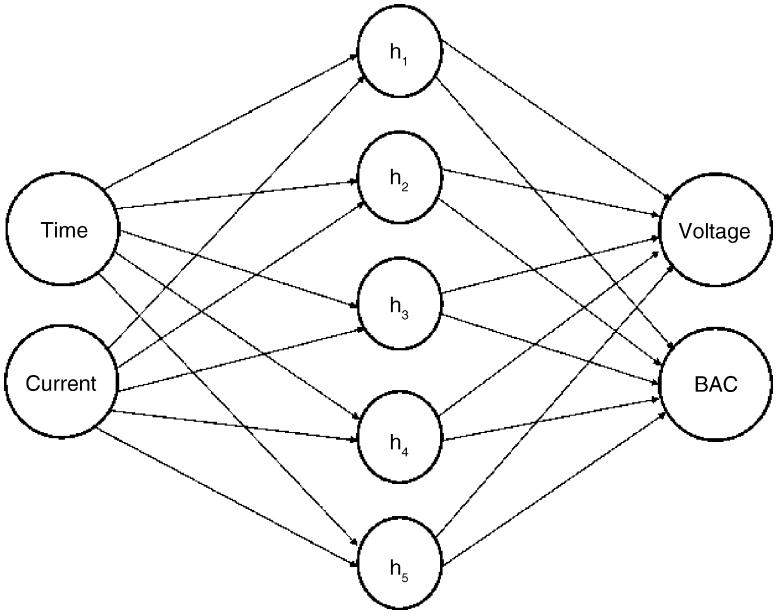

Fig. 7. The artificial neural network scheme: Time and current are inputs; h_1, h_2, h_3, h_4 and h_5 are nodes of hidden layer; voltage and BAC are outputs.

175 and 300 mA g^{-1}, respectively, confirm the ability of the ANN model to predict voltage.

Fig. 11(a and b) show the predicted BAC versus the corresponding experimental data at discharge currents of 175 and 300 mA g^{-1} in the validation set. As seen in Fig. 11(a and b), the correlation coefficients of 0.9974 and 0.9987 for discharge currents of 175 and 300 mA g^{-1} show that there is excellent agreement between experimental and prediction data.

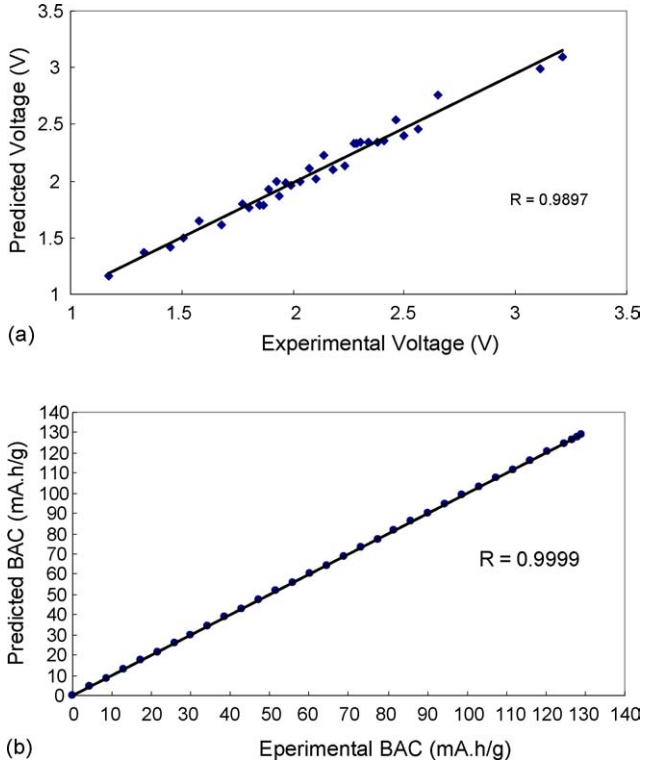

Fig. 8. Predictive ability of the proposed model for a typical discharge current of 250 mA g^{-1} in the training set: (a) variation of predicted voltage vs. experimental voltage and (b) variation of predicted BAC vs. experimental BAC.

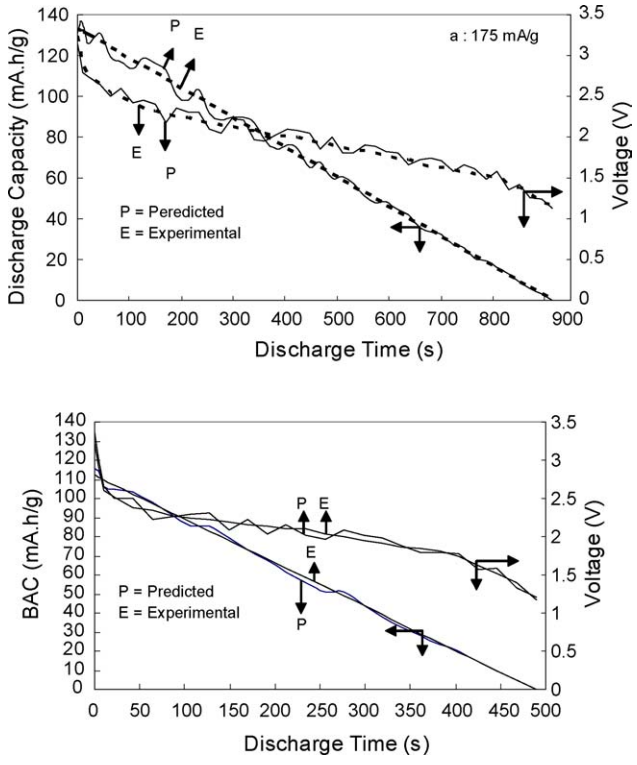

Fig. 9. Predictive ability of the proposed model for the prediction of voltage and BAC in the validation set at discharge currents of: (a) 175 mA g^{-1} and (b) 300 mAh g^{-1} at room temperature.

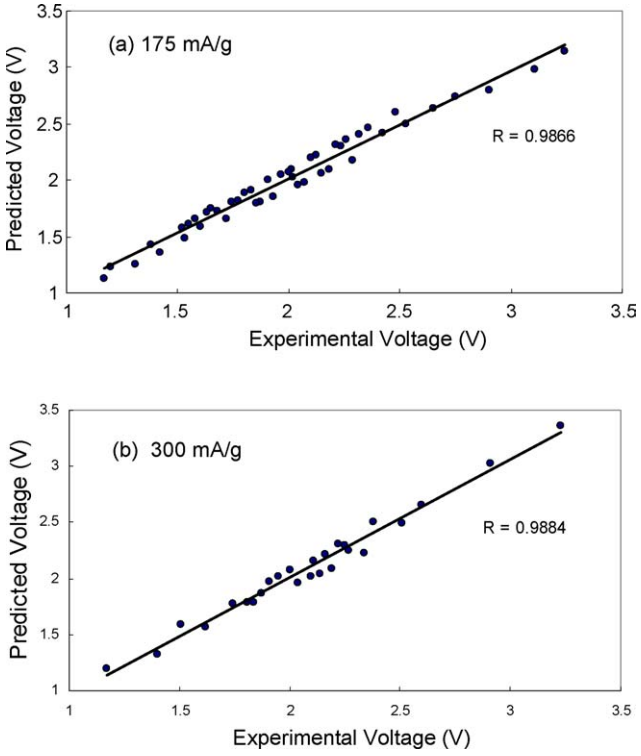

Fig. 10. Plot of predicted voltage vs. corresponding experimental voltage at discharge currents of: (a) 175 mA g^{-1} and (b) 300 mA g^{-1}.

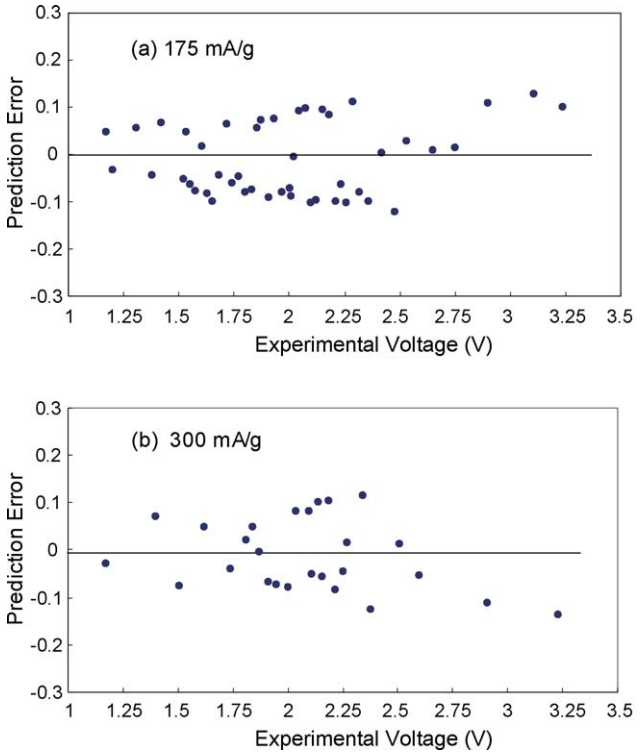

Fig. 12. Variation of prediction error with respect to the corresponding experimental voltage at discharge currents of: (a) 175 mA g^{-1} and (b) 300 mA g^{-1}.

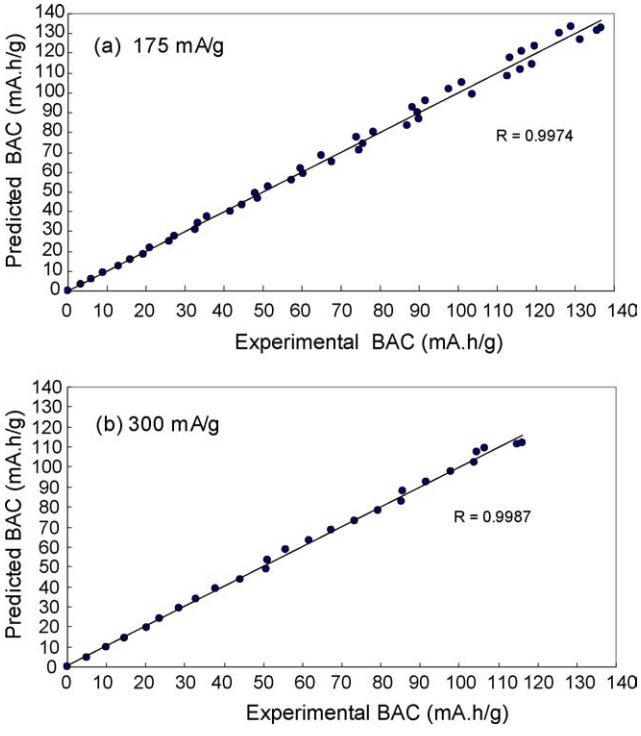

Fig. 11. Plot of predicted BAC vs. corresponding experimental BAC at discharge currents of: (a) 175 mA g^{-1} and (b) 300 mA g^{-1}.

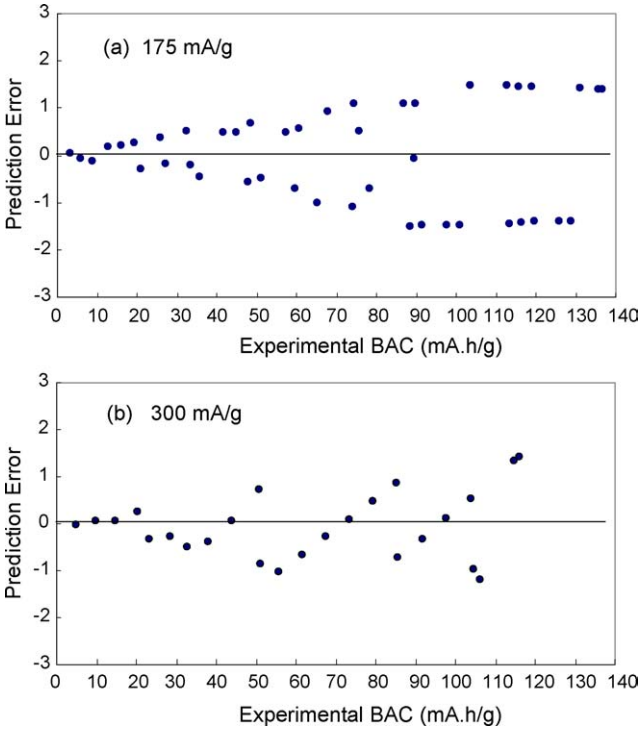

Fig. 13. Variation of prediction error with respect to the corresponding experimental BAC at discharge currents of: (a) 175 mA g^{-1} and (b) 300 mA g^{-1}.

The number of prediction errors with respect to the corresponding experimental data of voltage at discharge currents of 175 and 300 mA g^{-1} are shown in Fig. 12(a and b). As seen in Fig. 12(a and b), the proposed model can be used to predict voltage at different discharge currents with a very low mean prediction error. The percent of maximum prediction error for voltage at discharge currents of 175 and 300 mA g^{-1} are 3.94% and 4.18%, respectively.

Fig. 13(a and b) shows the prediction errors for BAC at discharge currents of 175 and 300 mA g^{-1} versus the corresponding experimental BAC data. As seen in Fig. 13(a and b), the proposed ANN model can be successfully employed in the prediction of BAC at different current and time of discharge. The percent of maximum prediction error for the prediction of BAC at discharge currents of 175 and 300 mA g^{-1} are 1.15% and 1.22%, respectively.

4. Conclusions

Polyaniline doped with perchloric acid possesses good conductivity and relatively high reversibility with respect to the redox reactions. Perchlorate doped polyaniline was highly efficient as a cathode material in rechargeable batteries. The use of optalloy in the zinc anode increased the overvoltage of hydrogen gas release.

The use of bipolar design in polyaniline batteries is quite new and useful. In this work, single-side metallized CDPE foil was used as a suitable conductive substrate in the construction of zinc-polyaniline bipolar electrodes. The proposed bipolar batteries are inexpensive, simple and possess high capacity and high columbic efficiency. The wet Zn-polyaniline batteries had a longer cycle life than the corresponding dry batteries.

ANN modeling was successfully used for the simultaneous modeling and prediction of voltage and BAC at different currents and times of discharge in Zn-polyaniline bipolar rechargeable batteries with a very low prediction error.

Acknowledgement

We gratefully acknowledge the support of this work by the Tarbiat Modarres University (T.M.U.) Research Council.

References

[1] A. Mirmohseni, R. Solhjoo, Eur. Polym. J. 39 (2003) 219.
[2] A.A. Syed, M.K. Dinesan, Talanta 38 (1991) 815.
[3] P. Novak, K. Muller, K.S.V. Santhanam, O. Haas, Chem. Rev. 97 (1997) 207.
[4] A. Kitani, M. Kaya, K. Sasaki, J. Electrochem. Soc. 133 (1986) 1069.
[5] N. Camaioni, G. Gasalbore-Miceli, W.A. Gazotti Jr., M.A. De Paoli, M. Fichera, Synth. Met. 90 (1997) 31.
[6] E. Spila, S. Panero, B. Scrosati, Electrochim. Acta 43 (1998) 1651.
[7] B. Wang, G. Li, F. Wang, J. Power Sources 24 (1988) 115.
[8] F. Trinidal, M.C. Montemayor, E. Fatas, J. Electrochem. Soc. 138 (1991) 3186.
[9] M. Sima, T. Visan, M. Buda, J. Power Sources 56 (1995) 133.
[10] G. Mengoli, M.M. Musiani, D. Pletcher, S. Valcher, J. Appl. Electrochem. 17 (1987) 525.
[11] W. Boachen, L. Gi, L. Changzhi, W. Fosong, J. Power Sources 24 (1988) 115.
[12] H. Karami, M.F. Mousavi, M. Shamsipur, J. Power Sources 124 (2003) 303.
[13] K. Wiesener, D. Ohms, G. Benczŭi-Ürmossy, M. Berthold, F. Haschka, J. Power Sources 84 (1999) 248.
[14] W.H. Kao, J. Power Sources 70 (1998) 8.
[15] M. Sakes, C. Kleijnen, D. Schmal, P.T. Have, J. Power Sources 95 (2001) 68.
[16] D. Ohms, M. Kohlhase, G. Benczŭi-Ürmossy, G. Schaedlich, K. Wiesenes, J. Harmel, J. Power Sources 96 (2001) 76.
[17] K. Ellis, A. Hill, J. Hill, A. Loyns, T. Partington, J. Power Sources 136 (2004) 366.
[18] P.A. Barbic, L. Binder, S. Voss, F. Hofer, W. Grogger, J. Power Sources 79 (1999) 271.
[19] M. Ghaemi, Ph.D. Dissertation, Technical University of Graz, Austria, 1995.
[20] M. Ghaemi, R. Amrollahi, F. Ataherian, Z. Kassae, J. Power Sources 117 (2003) 233.
[21] J.O. Bensenhard, M. He, J. Huslage, U. Krebber, J. Power Sources 44 (1993) 493.
[22] L. Binder, P.A. Barbic, S. Vo, F. Hofer, W. Grogger, Electrochem. Soc. Proc. 97 (1997) 933.
[23] M.S. Rahmanifar, M.F. Mousavi, M. Shamsipur, J. Power Sources 110 (2002) 229.
[24] H. Karami, M.F. Mousavi, M. Shamsipur, J. Power Sources 117 (2003) 255.
[25] P. Hagan, D. Fellowes, J. Power Sources 122 (2003) 77.
[26] P.E. Pascoe, J. Power Sources 45 (2004) 1015.
[27] S.K. Song, J. Power Sources 70 (1998) 157.
[28] P.E. Pascoe, A.H. Anbuky, Energy. Convers. Manage. 45 (2004) 277.
[29] A.J. Salkind, C. Fennie, P. Singh, T. Atwater, D.E. Reisner, J. Power Sources 80 (1999) 293.
[30] W.X. Shen, C.C. Chan, E.W.C. Lo, K.T. Chau, Energy. Convers. Manage. 43 (2002) 817.
[31] D. Baret, A. Vervaet, Electrochim. Acta 44 (1999) 3491.
[32] W.X. Shen, C.C. Chan, E.W.C. Lo, K.T. Chau, J. Power Sources 103 (2002) 180.
[33] W.L. Xing, X.W. He, Anal. Chim. Acta 349 (1997) 283.
[34] M.T. Hagan, H.B. Demuth, M. Beal, Neural Network Design, PWS, Boston, 1996.
[35] S. Haykin, Neural Network, Prentice-Hall, Englewood Cliffs, NJ, 1994.
[36] N.K. Bose, P. Liang, Neural Network Fundamentals, McGraw-Hill, New York, 1996.
[37] D.W. Patterson, Artificial Neural Networks: Theory and Applications, Simon and Schuster, New York, 1996.
[38] J. Zupan, J. Gasteiger, Anal. Chim. Acta 248 (1991) 1.
[39] A. Urbina, T.L. Paez, R.G. Jungst, B.Y. Liaw, J. Power Sources 110 (2002) 430.
[40] F. Giraud, Z.M. Salameh, Electr. Power Syst. Res. 50 (1999) 155.
[41] M. Urquidi-Macdonald, N.A. Bomberger, J. Power Sources 74 (1998) 87.
[42] J. Kan, H. Xue, S. Mu, J. Power Sources 74 (1998) 113.
[43] M. Ghorbani, M. Mazaheri, K. Khangholi, Y. Kharazi, Surf. Coat. Technol. 148 (2001) 71.
[44] S.M. Ahmed, Eur. Polym. J. 38 (2002) 1151.
[45] R. Mazeikiene, A. Malinauskas, Eur. Polym. J. 38 (2002) 1947.